# Mutational analysis of the Lem3p-Dnf1p putative phospholipid-translocating P-type ATPase reveals novel regulatory roles for Lem3p and a carboxyl-terminal region of Dnf1p independent of the phospholipid-translocating activity of Dnf1p in yeast

Takehiro Noji[a, b], Takaharu Yamamoto[a, *], Koji Saito[a], Konomi Fujimura-Kamada[a], Satoshi Kondo[b], and Kazuma Tanaka[a, *]

[a]Division of Molecular Interaction, Institute for Genetic Medicine, and [b]Department of Surgical Oncology, Hokkaido University Graduate School of Medicine, N15 W7, Kita-ku, Sapporo, 060-0815, Japan

[*]Corresponding authors

Fax: +81-11-706-7821

E-mail addresses: T. Yamamoto, yamata@igm.hokudai.ac.jp; K. Tanaka, k-tanaka@igm.hokudai.ac.jp

**Abstract**

Lem3p-Dnf1p is a putative aminophospholipid translocase (APLT) complex that is localized to the plasma membrane; Lem3p is required for Dnf1p localization to the plasma membrane. We have identified *lem3* mutations, which did not affect formation or localization of the Lem3p-Dnf1p complex, but caused a synthetic growth defect with the null mutation of *CDC50*, a structurally and functionally redundant homologue of *LEM3*. Interestingly, these *lem3* mutants exhibited nearly normal levels of NBD-labeled phospholipid internalization across the plasma membrane, suggesting that Lem3p may have other functions in addition to regulation of the putative APLT activity of Dnf1p at the plasma membrane. Similarly, deletion of the COOH-terminal cytoplasmic region of Dnf1p affected neither the localization nor the APLT activity of Dnf1p at the plasma membrane, but caused a growth defect in the *cdc50Δ* background. Our results suggest that the Lem3p-Dnf1p complex may play a role distinct from its plasma membrane APLT activity when it substitutes for the Cdc50p-Drs2p complex, its redundant partner in the endosomal/*trans*-Golgi network compartments.

## Introduction

Most cell types display an asymmetric distribution of phospholipids across the plasma membrane [1-3]. In general, the aminophospholipids phosphatidylserine (PS) and phosphatidylethanolamine (PE) are enriched in the inner leaflet facing the cytoplasm, whereas phosphatidylcholine (PC), sphingomyelin, and glycolipids are predominantly found in the outer leaflet of the plasma membrane. The inward transport of aminophospholipids is performed by an aminophospholipid translocase (APLT) or a flippase, one example of which is the type 4 P-type ATPase [4]. In humans, a few biological disorders have been linked or attributed to genes from this subfamily. FIC1 (ATP8B) mutations cause familial intrahepatic cholestasis, a defect in bile secretion [5, 6]. The ATP10C gene has been linked to Angelman syndrome and autism in some patients [7, 8]. However, little is known about the detailed cellular function of type 4 P-type ATPases, including these gene products. In *Saccharomyces cerevisiae*, a eukaryotic model organism, there are five type 4 P-type ATPases: Drs2p, Neo1p, Dnf1p, Dnf2p, and Dnf3p [9, 10]. Dnf1p and Dnf2p are primarily localized to the plasma membrane, and loss of both proteins causes a defect in the uptake of 7-nitrobens-2-oxa-1, 3-diazol-4-yl (NBD)-labeled PE, PC, and PS across the plasma membrane [10]. Drs2p localizes to endosomes and the *trans*-Golgi network (TGN), and has been implicated in the formation of transport vesicles from the TGN [9, 11]. Cdc50p, a member of the conserved membrane-spanning protein family, was identified as a gene required for polarized cell growth [12]. Cdc50p and its homolog, Lem3p, were subsequently shown to associate with Drs2p and Dnf1p, respectively, and to be required for the exit of these P-type ATPases from the endoplasmic reticulum (ER) [13]. Thus, disruption of the *LEM3* gene results in a marked decrease in the internalization of fluorescence-labeled analogs of PE and PC across the plasma membrane [13-15]. The Lem3p-Dnf1p and Cdc50p-Drs2p complexes are functionally redundant, because simultaneous

loss of function of both complexes results in a synthetic growth defect.

Colocalization and formation of a Lem3p-Dnf1p complex at the plasma membrane suggest that Lem3p possesses a function in the mature complex, in addition to its role in exit from the ER. In order to explore these functions of Lem3p, we isolated novel *lem3* point mutants that exhibited normal polarized localization of Dnf1p-EGFP from a collection of *lem3* mutants that exhibited synthetic growth defects with the *cdc50Δ* mutation. We also found that a COOH-terminal deletion mutant of Dnf1p exhibited phenotypes similar to those of the *lem3* mutants. These results suggest that Lem3p and the COOH-terminal domain of Dnf1p may have a function in utilization of the putative APLT activities of Dnf1p and Drs2p for the formation of transport vesicles from the TGN or endosomes.

**Materials and methods**

*Media and genetic techniques.* Yeast strains and plasmids used in this study are summarized in Tables 1 and 2, respectively. *Escherichia coli* DH5α and XL1-Blue were used for construction and amplification of plasmids. Unless otherwise specified, strains were grown in YPDA rich medium (1% yeast extract [Difco, Detroit, MI], 2% bacto-peptone [Difco], 2% glucose, and 0.01% adenine). Strains carrying plasmids were selected in synthetic medium (SD) containing the required nutritional supplements [16]. For induction of the *GAL1* promoter, 3% galactose and 0.2% sucrose were used as carbon sources, instead of glucose (YPGA). SDA plates containing 0.1% 5-fluoroorotic acid (5-FOA; Wako Pure Chemicals, Osaka, Japan; SDA+5-FOA plates) were used to counterselect for the presence of *URA3*-containing plasmids. Standard genetic manipulations of yeast were performed as described previously [17]. Yeast transformations were performed using the lithium acetate method [18, 19].

*Antibodies.* Mouse anti-HA (HA.11) and anti-Myc (9E10) monoclonal antibodies

were purchased from Babco (Richmond, CA) and Sigma-Aldrich (St. Louis, MO), respectively. Rabbit anti-Lem3p polyclonal antibodies have been described previously [14]. The horseradish peroxidase-conjugated secondary antibodies (sheep anti-mouse IgG and donkey anti-rabbit IgG) used for immunoblotting were purchased from Amersham Biosciences (Piscataway, NJ).

*Isolation of lem3 mutants.* To isolate *lem3* mutants, the *LEM3* gene was mutagenized by a PCR-based method [20]. The *LEM3* gene with multi-cloning site-flanking regions at both ends was amplified using primers pRS-F (5' GGCCCACTACGTGAACCATC 3') and pRS-R (5' TGAGCGAGGAAGCGGAAGAG 3') and the plasmid pRS316-LEM3 (pKT1252) as a templete. The reaction mixture (1 ng/µl pRS316-LEM3, 1 µM primers, 10 mM Tris·HCl pH 8.3, 50 mM KCl, 2.5 mM $MgCl_2$, 0.5 mM $MnCl_2$, 0.2 mM dATP, 0.2 mM dGTP, 1 mM dCTP, 1 mM dTTP, and 0.05 U/µl *Taq* polymerase [Sigma-Aldrich]) was subjected to 30 cycles of amplification (94°C, 1 min; 50°C, 1 min; 72°C, 3 min), followed by a 10-min incubation at 72°C. The PCR-amplified fragment was isolated by ethanol precipitation and mixed with pRS315 linearized by digestion with BamHI and XhoI. This DNA mixture was introduced into a *cdc50Δ lem3Δ crf1Δ* strain expressing *DNF1* tagged with enhanced green fluorescent protein (EGFP) and harboring pRS316-LEM3 (YKT1121) to allow homologous recombination between the PCR product and the linearized vector plasmid. Transformants were selected on SD-Leu. After incubation at 30°C for 2 days, the resulting colonies were replica-plated on SDA+5-FOA plates to select for the loss of *URA3*-containing pRS316-LEM3. The $LEU^+$ $URA^-$ clones were examined for growth at 30°C and 37°C on YPDA plates, and for Dnf1p-EGFP localization.

*Construction of dnf1 COOH-terminal deletion mutants.* Deletion mutants of the *DNF1* COOH-terminal cytoplasmic domain were constructed on our strain background by PCR-based procedures as described previously [21].

*Immunoprecipitation and western blotting.* The preparation of crude membrane

fractions was performed as described previously [13]. For immunoprecipitation, membrane fractions were prepared from 200 $OD_{600}$ of cells and were solubilized in 0.8 ml of immunoprecipitation buffer (10 mM Tris·HCl pH 7.5, 150 mM NaCl, 2 mM EDTA, and 1% CHAPS) containing protease inhibitors (1 µg/ml aprotinin, 1 µg/ml leupeptin, 1 µg/ml pepstatin, 2 mM benzamidine, and 1 mM phenylmetylsulfonylfluoride). Insoluble material was removed by centrifugation at 20,630 x *g* for 5 min at 4°C. The cleared lysates were split into two aliquots, which were incubated either with 5 µg of anti-Myc antibody or control mouse IgG for 1 h at 4°C. These samples were rotated with 10 µl of protein G-Sepharose 4 Fast Flow (Amersham Biosciences AB, Uppsala, Sweden) for 1 h at 4°C. The protein G-Sepharose beads were then pelleted and washed three times with immunoprecipitation buffer in the absence of detergents. The immunoprecipitates were separated by SDS-PAGE and transferred to polyvinylidene difluoride membrane. Western blotting was performed as described previously [13].

*Detergent-insoluble glycolipid-enriched complexes (DIG) isolation*. Spheroplasts were prepared as described previously [22]. The isolation of DIG was performed as described previously [23].

*Internalization of fluorescence-labeled phospholipids into yeast cells*. 1-palmitoyl-2-(6-NBD-aminocaproyl)-PE (NBD-PE), 1-palmitoyl-2-(6-NBD-aminocaproyl)-PC (NBD-PC), and dioleoylphosphatidylcholine (DOPC) were obtained from Avanti Polar Lipids (Alabaster, AL). The preparation of large unilamellar vesicles was performed as described previously [13]. Fluorescently labeled phospholipid internalization experiments were performed as described previously [13, 14]. Briefly, cells carrying the designated plasmids were grown to early-mid log phase in SD-Leu media at 30°C or 37°C. After dilution to 0.35 $OD_{600}$/ml in SD-Leu, cells were incubated with vesicles containing 40% NBD-phospholipids and 60% DOPC at a final concentration of 50 µM, and shaken for 30 min at 30°C or 37°C. Cells were then suspended in SD medium containing 0.01% $NaN_3$ and 2.5 µg/ml propidium iodide (PI) to

allow the exclusion of PI-positive dead cells in flow cytometric analysis. Flow cytometry of NBD-labeled cells was performed on a FACS Calibur cytometer using CellQuest software (BD Biosciences, San Jose, CA). Green fluorescence of the NBD was plotted on a histogram to allow calculation of the mean fluorescence intensity.

*Microscopic observations*. Cells were observed using a Nikon ECRIPSE E800 microscope (Nikon Instec, Tokyo, Japan) equipped with an HB-10103AF super high-pressure mercury lamp and a 1.4 numerical aperture 100x Plan Apo oil immersion objective (Nikon Instec) with the appropriate fluorescence filter sets (Nikon Instec) and differential interference contrast (DIC) optics. Images were acquired with a digital cooled charge-coupled device camera (C4742-95-12NR; Hamamatsu Photonics, Hamamatsu, Japan) using AQUACOSMOS software (Hamamatsu Photonics). Observations were compiled from the examination of at least 100 cells. To visualize GFP-tagged proteins in living cells, cells were grown to early-mid log phase, harvested, and resuspended in SD medium. Cells were mounted on microslide glass and observed immediately using a GFP bandpass filter set. Cells with small buds, defined to be no greater than 30% the size of the mother cell, were examined to quantify the Dnf1p and Dnf2p polarity.

**Results**

*Isolation of lem3 mutations that affect the growth of the cdc50Δ mutant but not the localization of Dnf1p*

Lem3p associates not only with Dnf1p, but also with Dnf2p, and is required for the ER exit of Dnf2p (our unpublished results). Crf1p, the third member of the Cdc50p family, makes a minor contribution to the cell growth compared to Cdc50p and Lem3p: the *cdc50Δ lem3Δ* mutant exhibits a severe growth defect, whereas the *cdc50Δ lem3Δ*

*crf1Δ* mutant is lethal [13].

To determine whether Lem3p has any functions other than the ER exit and plasma membrane localization of Dnf1p and Dnf2p, we attempted to isolate *lem3* mutants that showed temperature-sensitive growth in the absence of both *CDC50* and *CRF1*, but exhibited the normal polarized localization of Dnf1p-EGFP. A plasmid-borne *LEM3* gene was randomly mutagenized by a PCR-based method and introduced into a *cdc50Δ lem3Δ crf1Δ DNF1-EGFP* (YKT1121) strain as described in Materials and methods. From $1.2x10^4$ initial transformants, 178 temperature-sensitive mutants were isolated. The plasmids containing *lem3* alleles were recovered, introduced into the *lem3Δ* mutant, and examined for Dnf1p-EGFP localization. As a result, we isolated three mutants (*lem3-50*, *lem3-112*, and *lem3-116*) that had nearly normal localization of Dnf1p-EGFP (Fig. 2A and our unpublished results). However, these three mutants exhibited poor growth even at 30°C (see below). We were not able to examine the localization of mutant Lem3ps, because tagging Lem3p at either the $NH_2$ or COOH terminus impairs its function ([13] and our unpublished results). However, it is likely that the mutant Lem3ps localized to the polarized site with Dnf1p-EGFP, since formation of the Lem3p-Dnf1p complex is prerequisite for ER exit and normal localization of Dnf1p [13]. We re-examined the effects of these *lem3* mutations on the growth of *cdc50Δ crf1Δ* mutant cells. Since the poor growth phenotype of the *cdc50Δ* mutant easily reverts when transformed (our unpublished results), we utilized strains expressing *CDC50* under the control of the glucose-repressible *GAL1* promoter in the subsequent experiments. The three *lem3* mutations led to a growth defect at both 30°C and 37°C in a $P_{GAL1}$-*CDC50 crf1Δ* strain on glucose-containing plates (Fig. 1A). Sequencing of the *lem3* alleles identified four amino acid substitutions in each of *lem3-50*, *lem3-112*, and *lem3-116* (Fig. 1B). Notably, in the Lem3-112 mutant protein, the tryptophan at amino acid position 316, which is evolutionarily conserved from yeast to mammals in the Cdc50p family (Fig. 1C), was substituted for arginine. We constructed this point

mutation in *LEM3* (*lem3(R316W)*), and it also led to poor growth at both 30°C and 37°C in the *cdc50Δ crf1Δ* background (Fig. 1A). The *lem3(R316W)* mutant was chosen for further characterization.

We more precisely determined the localization of Dnf1p-EGFP in small-budded cells of *lem3-116, lem3(R316W),* or *lem3-112* mutant strain (Fig. 2A). In the *LEM3* strain, Dnf1p-EGFP was found in small punctate structures underlying the plasma membrane and concentrated to the polarized site of growth in about 90% of small-budded cells as described previously [9, 10, 13]. The localization of Dnf1p-EGFP in the *lem3(R316W)* and *lem3-116* mutants was similar to that in the *LEM3* strain at 30°C, whereas the ratio of polarized distribution slightly decreased at 37°C. However, in about 40% or 60% of *lem3-112* cells, Dnf1p-EGFP was localized in the ER or diffused throughout the cytoplasm at 30°C or 37°C, respectively (Fig. 2B). Dnf2p-EGFP was also localized to the polarized sites in the *LEM3* cells (Fig. 2B) and its localization was examined in the *lem3* mutants. In almost all *lem3-116, lem3(R316W)*, and *lem3-112* mutant cells, localization of Dnf2p-EGFP exhibited an ER pattern at both 30°C and 37°C (Supplemental data 1 and Fig. 2B). The *dnf1Δ* mutation caused a growth defect in the *cdc50Δ* or *drs2Δ* mutant, but the *dnf2Δ* mutation did not ([9, 13] and our unpublished results), indicating that *DNF2* makes little contribution to cell growth in the absence of *CDC50*. Thus, it seems that the *lem3* mutants are also defective in the Dnf1p-related functions.

To examine whether Lem3p(R316W) physically interacts with Dnf1p or Dnf2p by coimmunoprecipitation experiments, we constructed a *lem3Δ* strain that expresses a COOH-terminally 13Myc-tagged version of *DNF1* or *DNF2* and harbors a plasmid containing *LEM3* or *lem3(R316W)*. As shown in Fig. 3A, Lem3p(R316W) coimmunoprecipitated with Dnf1p-13Myc. Unexpectedly, Lem3p(R316W) also coimmunoprecipitated with Dnf2p-13Myc, suggesting that the Lem3p(R316W)-Dnf2p complex is formed in the ER, but is not transported out of the ER due to the action of the ER qual-

ity control mechanism. Kato et al. showed that Lem3p/Ros3p was associated with the detergent-insoluble fraction [14]. As shown in Fig. 3B, a significant portion of Lem3p(R316W), comparable to that of wild-type Lem3p, was present in the low density detergent-insoluble fractions (fraction number 1 to 3). Our results suggest that Lem3p(R316W) interacts with Dnf1p in a normal manner, is transported from the ER to the plasma membrane in a complex with Dnf1p, and associates with detergent-insoluble fractions.

*The lem3(R316W) mutation does not impair the putative APLT activity of Dnf1p*

Next, we analyzed whether the *lem3(R316W)* mutation affects the putative APLT activity of Dnf1p. In order to examine the effect of *lem3(R316W)* on Dnf1p only, we measured NBD-labeled phospholipid internalization in the *dnf2Δ* strain. As shown in Fig. 4A, the *dnf2Δ* mutation caused a 30-40% reduction in the internalization of NBD-PE and -PC. The *lem3(R316W)* mutation did not affect either NBD-PE or -PC internalization in the *dnf2Δ* background. Similar results were obtained when these experiments were performed at 37°C. These results suggest that the R316W substitution of Lem3p does not affect the APLT activity of Dnf1p. The *lem3-112* mutation reduced NBD-PE and -PC internalization, although its effects were mild compared with those of the *lem3Δ* mutation. This partial reduction of NBD-labeled phospholipid internalization may be due to partial defects in the localization of Dnf1p-EGFP to the plasma membrane in the *lem3-112* mutant (Fig. 2B). If this is the case, Lem3-112p may not affect APLT activity when it is associated with Dnf1p.

Cinnamycin (Ro 09-0198) is a 19-amino acid tetracyclic polypeptide that forms a tight equimolar complex with PE in biological membranes [24]. *lem3* and *dnf1Δ dnf2Δ* mutants, but not the *dnf1Δ* or *dnf2Δ* single mutant, are hypersensitive to cinnamycin [10, 14], consistent with the defects in NBD-PE internalization in these mutants.

Duramycin closely resembles cinnamycin [25], and we found that it also inhibited the growth of the *lem3Δ* strain. As shown in Fig. 4B, the *lem3-112* mutant was partially sensitive to duramycin, whereas *lem3(R316W)* and *lem3-116* mutants were resistant. Taken together, these results suggest that the *lem3(R316W)* mutation does not impair the putative APLT activity of Dnf1p.

*The COOH-terminal deletion of Dnf1p does not impair its putative APLT activity*

Recent studies from the Jackson group have indicated that the COOH-terminal cytoplasmic tail of Drs2p is essential for its function, and has a function independent of the ATPase domain [26]. We examined the effects of COOH-terminal deletions on the function and putative APLT activity of Dnf1p. We constructed three deletion mutants of *DNF1* in its COOH-terminal tail (*dnf1Δ(1403-1571), dnf1Δ(1465-1571),* and *dnf1Δ(1523-1571)*) tagged with *EGFP* or *HA* (Supplemental data 2A).

The localization of Dnf1pΔ(1465-1571)-EGFP and Dnf1pΔ(1523-1571)-EGFP was indistinguishable from that of wild-type Dnf1p-EGFP, but Dnf1pΔ(1403-1571)-EGFP was localized to the ER (Fig. 5A and Supplemental data 2B). Interestingly, the *dnf1Δ(1465-1571)-3HA* mutation, but not the *dnf1Δ(1523-1571)-3HA* mutation, led to a weak synthetic growth defect in Cdc50p-depleted cells (Fig. 5B and Supplemental data 2C). The 1523-1571 region of Dnf1p, however, may have a function, because the EGFP-tagged *dnf1Δ(1523-1571)* mutation, but not wild-type *DNF1-EGFP,* led to a synthetic growth defect in Cdc50p-depleted cells (Supplemental data 2C).

Since Dnf1pΔ(1465-1571)-EGFP exhibited normal polarized localization, but was defective for growth when Cdc50p was depleted, we examined internalization of NBD-labeled PC and PE in *dnf1Δ(1465-1571)-3HA* mutants. We confirmed that the expression of Dnf1pΔ(1465-1571)-3HA was slightly lower, but comparable, to that of wild-type Dnf1p-3HA (our unpublished results). As shown in Fig. 5C, the *dnf1Δ(1465-*

*1571)-3HA dnf2Δ* mutant was insensitive to 5 μM duramycin, similar to the *DNF1-3HA dnf2Δ* or *dnf2Δ* mutant (our unpublished results). Consistently, in the *dnf1Δ(1465-1571)-3HA* mutant, NBD-PE and -PC internalization was comparable to that in the wild-type, and, surprisingly, in the *dnf2Δ* background, the *dnf1Δ(1465-1571)-3HA* mutation increased both NBD-PE and -PC internalization (Fig. 5D). These results suggest that the COOH-terminal cytoplasmic region of Dnf1p plays an important role, in a manner independent of the regulation of the putative APLT activity, in Dnf1p function that is redundant with that of the Cdc50p-Drs2p complex.

**Discussion**

In this study, we have genetically demonstrated that Lem3p possesses functions in the mature Lem3p-Dnf1p complex, in addition to its role in the ER exit of Dnf1p. We have previously made similar observations with the COOH-terminally HA-tagged version of *LEM3*: although Lem3p-HA was normally localized to the plasma membrane and formed a complex with Dnf1p, *lem3-HA* caused synthetic poor growth with the *cdc50Δ* mutation [13]. In addition, the *lem3-HA* mutant normally internalized NBD-PE and -PC (our unpublished results).

The vertebrate plasma membrane $Na^+$, $K^+$-ATPase is composed of catalytic α- and noncatalytic β-subunits. The β-subunit is likely required not only for transport out of the ER, but also for regulation of the $Na^+$, $K^+$-pump transport activity of the mature complex [27]. Interestingly, the *lem3(R316W)* mutant, which displayed normal polarized localization of Dnf1p-EGFP, was not impaired in its uptake of NBD-PE and -PC, suggesting that Lem3p(R316W) is defective in harnessing the putative APLT activity of Dnf1p for intracellular functions shared by Cdc50p-Drs2p. It is, however, also possible that Lem3p has functions independent of the APLT activity of Dnf1p, although we do not have evidence that Lem3p dissociates from Dnf1p after the ER exit of the com-

plex.

Since *lem3* mutations isolated in this study exhibited synthetic growth defects with the *cdc50Δ* mutation, these *lem3* mutants may be defective in functions regulated by the Cdc50p-Drs2p complex. Consistently, simultaneous overexpression of *LEM3* and *DNF1* suppressed the growth defects of the *cdc50Δ* mutant (Supplemental data 3). Cdc50p and Drs2p, which are localized to endosomal/TGN compartments, have been suggested to function in vesicular trafficking at these compartments. *DRS2*, which was first isolated as a mutation that is synthetically lethal with a mutation in *ARF1* encoding the Arf1p (ADP-ribosylation factor) small GTPase, has been implicated in the formation of clathrin-coated vesicles from the TGN [11]. Cdc50p has been shown to be involved in endocytic recycling of Snc1p, an exocytotic v-SNARE [13]. Dnf1p-EGFP localizes not only at the plasma membrane, but also in internal punctate structures (Fig. 2A and [10, 13]), which may represent endosomal/TGN compartments. Consistently, Dnf1p-EGFP lost its intracellular localization and accumulated at the plasma membrane in the endocytosis-deficient *vrp1Δ* mutant cells [13]. In addition, Dnf1p-EGFP accumulated intracellularly in *cdc50* mutant cells as was GFP-Snc1p [13]. The involvement of Dnf1p and Dnf2p in endocytic recycling was suggested by the observation that GFP-Snc1p accumulated intracellularly in the *dnf1Δ dnf2 Δ dnf3Δ* mutant [9], consistent with our observation that simultaneous overexpression of *LEM3* and *DNF1* partially suppressed the cytoplasmic accumulation of Snc1p at 30°C in *cdc50Δ* mutant cells (our unpublished results).

One proposed role for the phospholipid asymmetry generated by APLT is to recruit machinery for vesicle formation to the membrane [28]. Thus, one interesting possibility for the function of Lem3p and Cdc50p may be that these proteins regulate tethering of proteins required for vesicle budding to APLT complexes to promote vesicle formation at a localized region of endosomal/TGN membranes. Since the *dnf1Δ(1465-1571)* mutant exhibited phenotypes similar to those of the *lem3(R316W)* mutant, the COOH-

terminal 1465-1571 region of Dnf1p may be implicated in similar functions. Recently, Drs2p has been reported to directly interact with Gea2p, an Arf GEF (guanine nucleotide exchange factor), and suggested to function as its receptor at the TGN [26]. The Gea2p-binding region was mapped to a 21-amino acid region of the COOH-terminal cytoplasmic tail in Drs2p, just upstream of a region highly conserved among all, including mammalian, Drs2p homologues. Since this region has some weak homology with the same region of Dnf1p, as Jackson and colleagues described, Gea2p may bind directly to the COOH-terminal cytoplasmic region of Dnf1p. It is an interesting possibility that the Cdc50p/Lem3p family members regulate the interaction of APLT with its binding partners, including Gea2p.

**Acknowledgments**

We would like to thank Masato Umeda for the anti-Lem3p-antibodies. We thank members of the Tanaka laboratory for valuable discussions. We also thank Eriko Itoh for technical assistance. T.N. is especially grateful to Yukari Noji for encouragement during this work. This work was supported by grants-in-aid for scientific research from the Ministry of Education, Culture, Sports, Science and Technology, Japan, and from Japan Society for the Promotion of Science to T.Y., K.S., K.F-K., and K.T.

**References**


[1] P.F. Devaux, Static and dynamic lipid asymmetry in cell membranes, Biochemistry 30 (1991) 1163-1173.

[2] J. Cerbon, and V. Calderon, Changes of the compositional asymmetry of phospholipids associated to the increment in the membrane surface potential, Biochim. Biophys. Acta 1067 (1991) 139-144.

[3] C. Diaz, and A.J. Schroit, Role of translocases in the generation of phosphatidylserine asymmetry, J. Membr. Biol. 151 (1996) 1-9.

[4] J.C. Holthuis, and T.P. Levine, Lipid traffic: floppy drives and a superhighway, Nat. Rev. Mol. Cell Biol. 6 (2005) 209-220.

[5] R. Thompson, and P.L. Jansen, Genetic defects in hepatocanalicular transport, Semin. Liver Dis. 20 (2000) 365-372.

[6] P. Ujhazy, D. Ortiz, S. Misra, S. Li, J. Moseley, H. Jones, and I.M. Arias, Familial intrahepatic cholestasis 1: studies of localization and function, Hepatology 34 (2001) 768-775.

[7] L.B. Herzing, S.J. Kim, E.H. Cook, Jr., and D.H. Ledbetter, The human aminophospholipid-transporting ATPase gene ATP10C maps adjacent to UBE3A and exhibits similar imprinted expression, Am. J. Hum. Genet. 68 (2001) 1501-1505.

[8] M. Meguro, A. Kashiwagi, K. Mitsuya, M. Nakao, I. Kondo, S. Saitoh, and M. Oshimura, A novel maternally expressed gene, ATP10C, encodes a putative aminophospholipid translocase associated with Angelman syndrome, Nat. Genet. 28 (2001) 19-20.

[9] Z. Hua, P. Fatheddin, and T.R. Graham, An essential subfamily of Drs2p-related P-type ATPases is required for protein trafficking between Golgi complex and endosomal/vacuolar system, Mol. Biol. Cell 13 (2002) 3162-3177.

[10] T. Pomorski, R. Lombardi, H. Riezman, P.F. Devaux, G. van Meer, and J.C.

Holthuis, Drs2p-related P-type ATPases Dnf1p and Dnf2p are required for phospholipid translocation across the yeast plasma membrane and serve a role in endocytosis, Mol. Biol. Cell 14 (2003) 1240-1254.

[11] C.Y. Chen, M.F. Ingram, P.H. Rosal, and T.R. Graham, Role for Drs2p, a P-type ATPase and potential aminophospholipid translocase, in yeast late Golgi function, J. Cell Biol. 147 (1999) 1223-1236.

[12] K. Misu, K. Fujimura-Kamada, T. Ueda, A. Nakano, H. Katoh, and K. Tanaka, Cdc50p, a conserved endosomal membrane protein, controls polarized growth in *Saccharomyces cerevisiae*, Mol. Biol. Cell 14 (2003) 730-747.

[13] K. Saito, K. Fujimura-Kamada, N. Furuta, U. Kato, M. Umeda, and K. Tanaka, Cdc50p, a protein required for polarized growth, associates with the Drs2p P-type ATPase implicated in phospholipid translocation in *Saccharomyces cerevisiae*, Mol. Biol. Cell 15 (2004) 3418-3432.

[14] U. Kato, K. Emoto, C. Fredriksson, H. Nakamura, A. Ohta, T. Kobayashi, K. Murakami-Murofushi, and M. Umeda, A novel membrane protein, Ros3p, is required for phospholipid translocation across the plasma membrane in *Saccharomyces cerevisiae*, J. Biol. Chem. 277 (2002) 37855-37862.

[15] P.K. Hanson, L. Malone, J.L. Birchmore, and J.W. Nichols, Lem3p is essential for the uptake and potency of alkylphosphocholine drugs, edelfosine and miltefosine, J. Biol. Chem. 278 (2003) 36041-36050.

[16] M.D. Rose, F. Winston, and P. Hieter, Methods in Yeast Genetics: A Laboratory Course Manual, Cold Spring Harbor Press, Cold Spring Harbor, 1990.

[17] C. Guthrie, and G.R. Fink, Guide to Yeast Genetics and Molecular Biology, Academic Press, San Diego, 1991.

[18] R. Elble, A simple and efficient procedure for transformation of yeasts, Biotechniques 13 (1992) 18-20.

[19] R.D. Gietz, and R.A. Woods, Transformation of yeast by lithium acetate/single-

stranded carrier DNA/polyethylene glycol method, Methods Enzymol. 350 (2002) 87-96.

[20] R.C. Cadwell, and G.F. Joyce, Randomization of genes by PCR mutagenesis, PCR Methods Appl. 2 (1992) 28-33.

[21] M.S. Longtine, A. McKenzie, 3rd, D.J. Demarini, N.G. Shah, A. Wach, A. Brachat, P. Philippsen, and J.R. Pringle, Additional modules for versatile and economical PCR-based gene deletion and modification in *Saccharomyces cerevisiae*, Yeast 14 (1998) 953-961.

[22] C.A. Kaiser, E.J. Chen, and S. Losko, Subcellular fractionation of secretory organelles, Methods Enzymol. 351 (2002) 325-338.

[23] M. Bagnat, S. Keranen, A. Shevchenko, A. Shevchenko, and K. Simons, Lipid rafts function in biosynthetic delivery of proteins to the cell surface in yeast, Proc. Natl. Acad. Sci. USA 97 (2000) 3254-3259.

[24] S.Y. Choung, T. Kobayashi, J. Inoue, K. Takemoto, H. Ishitsuka, and K. Inoue, Hemolytic activity of a cyclic peptide Ro09-0198 isolated from *Streptoverticillium*, Biochim. Biophys. Acta 940 (1988) 171-179.

[25] J. Navarro, J. Chabot, K. Sherrill, R. Aneja, S.A. Zahler, and E. Racker, Interaction of duramycin with artificial and natural membranes, Biochemistry 24 (1985) 4645-4650.

[26] S. Chantalat, S.K. Park, Z. Hua, K. Liu, R. Gobin, A. Peyroche, A. Rambourg, T.R. Graham, and C.L. Jackson, The Arf activator Gea2p and the P-type ATPase Drs2p interact at the Golgi in *Saccharomyces cerevisiae*, J. Cell Sci. 117 (2004) 711-722.

[27] K. Geering, A. Beggah, P. Good, S. Girardet, S. Roy, D. Schaer, and P. Jaunin, Oligomerization and maturation of Na,K-ATPase: functional interaction of the cytoplasmic $NH_2$ terminus of the β subunit with the α subunit, J. Cell Biol. 133 (1996) 1193-1204.

[28] T. Pomorski, J.C. Holthuis, A. Herrmann, and G. van Meer, Tracking down lipid

flippases and their biological functions, J. Cell Sci. 117 (2004) 805-813.

[29] R.S. Sikorski, and P. Hieter, A system of shuttle vectors and yeast host strains designed for efficient manipulation of DNA in *Saccharomyces cerevisiae*, Genetics 122 (1989) 19-27.

[30] R.D. Gietz, and A. Sugino, New yeast-*Escherichia coli* shuttle vectors constructed with *in vitro* mutagenized yeast genes lacking six-base pair restriction sites, Gene 74 (1988) 527-534.

**Figure legends**

Fig. 1. Effects of the newly isolated *lem3* mutations on the growth of the *cdc50Δ crf1Δ* mutant. (A) The $P_{GAL1}$-*CDC50 lem3Δ crf1Δ* (YKT1104) strain was transformed with YCplac111-LEM3 (pKT1483), YCplac111, YCplac111-lem3-50 (pKT1587), YCplac111-lem3-112 (pKT1585), YCplac111-lem3-116 (pKT1586), or YCplac111-lem3(R316W) (pKT1499). The transformants were cultured in YPDA media at 30°C for 12 h, serially diluted, and spotted onto YPGA or YPDA plates, followed by incubation at 30°C or 37°C for 19 h. (B) The amino acid substitutions identified in the *lem3-50* (open circles), *lem3-112* (inverted triangles), and *lem3-116* (rhombuses) mutants are depicted. The star indicates an amino acid position (R316) that is evolutionarily conserved from yeast to mammals. TM: predicted transmembrane domain. (C) Alignment of amino acid sequences adjacent to the conserved residue R316 of Lem3p and its homologous proteins from *S. cerevisiae* and other organisms. Black and gray boxes indicate identical and similar amino acids, respectively. The protein accession numbers are as follows: Lem3p (CAA96254), Cdc50p (CAA42249), Crf1p (CAA96329), nematoda (*Caenorhabditis elegans;* AAC48073), fly (*Drosophila melanogaster;* AAF48613), mouse (*Mus musculus;* AAH18367), and human (*Homo sapiens*; NP06717).

Fig. 2. The newly isolated *lem3* mutations do not affect the localization of Dnf1p-EGFP. (A) Localization of Dnf1p-EGFP in *lem3* mutants. The *lem3Δ DNF1-EGFP* (YKT773) strain was transformed with the plasmids used in Fig. 1A. The *DNF1-EGFP* (YKT771) strain was used as a control strain (WT). Cells were grown at 30°C to the log phase, and Dnf1p-EGFP was visualized using a GFP bandpass filter. (B) The Dnf1p-EGFP and Dnf2p-EGFP localization patterns and the percentage of cells exhibiting these patterns in *lem3* mutants. To examine the polarized Dnf1p-EGFP, strains described in (A) were used, while to examine the polarized Dnf2p-EGFP, the

*lem3Δ DNF2-EGFP* (YKT923) strains containing plasmids in Fig. 1A were used. The *DNF2-EGFP* (YKT1056) strain was used as a control (WT). Cells were grown and EGFP fusion proteins were visualized as in (A). More than one hundred small-budded cells were examined for each determination. The localization of Dnf1p-EGFP or Dnf2p-EGFP was categorized as localized to the polarized site (polarized; black), diffused intracellularly (diffuse; light gray), localized to both polarized sites and the ER (ER + polarized; dark gray), or localized to the ER (ER; blank). Representative images of each category are presented on the right side.

Fig. 3. The *lem3(R316W)* mutation does not affect the interaction with Dnf1p or Dnf2p, or the association with detergent-insoluble fractions. (A) Coimmunoprecipitation of Lem3p(R316W) with Dnf1p-13Myc (upper panel) or Dnf2p-13Myc (lower panel). The *lem3Δ DNF1-13MYC* (YKT1112) or the *lem3Δ DNF2-13MYC* (YKT1113) strain was transformed with plasmid YCplac111-LEM3 (pKT1483) or YCplac111-lem3(R316W) (pKT1499). Cells were grown at 30°C to a density of 0.5 $OD_{600}$/ml in YPDA medium. Membrane extracts were then prepared as described in Materials and methods. Myc-tagged P-type ATPases were immunoprecipitated with an anti-Myc antibody (9E10) from membrane extracts. Immunoprecipitates were subjected to SDS-PAGE, followed by immunoblot analysis using antibodies against Myc (top) and Lem3p (bottom). The results shown are representatives of several independent experiments. (B) Lem3p(R316W) as well as Lem3p is associated with low density detergent-insoluble fractions. Detergent-insoluble glycolipid-enriched complexes (DIGs) were isolated as described in Materials and methods. The presence of Lem3p (WT) or Lem3p(R316W) in each fraction collected from the top of the Opti-Prep density gradient (fraction number 1, top; fraction number 6, bottom) was examined by immunoblotting using the anti-Lem3p antibody. Tx; lysates treated with 1% Triton X-100.

Fig. 4. The *lem3(R316W)* mutation does not affect the putative APLT activity of

Dnf1p. (A) Internalization of NBD-labeled phospholipids in *lem3* mutants. The *lem3Δ* (YKT715) and *lem3Δ dnf2Δ* (YKT1111) mutants were transformed with plasmids containing either the wild-type or mutant *LEM3* gene. Cells were grown to the early-mid log phase in SD-Leu medium at 30°C or 37°C, followed by labeling with NBD-PE or -PC for 30 min at the same temperature. The percentage of average accumulation (±SD, three independent experiments) of the NBD-labeled phospholipid relative to the *lem3Δ* strain containing YCplac111-LEM3 is presented. Plasmids used were as follows: YCplac111-LEM3 (pKT1483), YCplac111 (Vector), YCplac111-lem3(R316W) (pKT1449), and YCplac111-lem3-112 (pKT1585). (B) Sensitivity of *lem3* mutants to duramycin. Wild-type (YKT38) or the *lem3Δ dnf2Δ* mutant (YKT1111) containing YCplac111-lem3-116 (pKT1586) or a plasmid described in (A) was streaked onto YPDA containing 5 μM duramycin, followed by incubation at 30°C for 2 days.

Fig. 5. Effects of deletion of the COOH-terminal cytoplasmic region of Dnf1p. (A) Localization of Dnf1pΔ(1465-1571)-EGFP. Cells were grown in YPDA media at 30°C to the log phase, and the EGFP-fused protein was visualized using a GFP bandpass filter. Strains examined were *DNF1-EGFP* (YKT771) and *dnf1Δ(1465-1571)-EGFP* (YKT1123). (B) The *dnf1Δ(1465-1571)* mutation led to synthetic poor growth in Cdc50p-depleted cells. Wild-type (WT, YKT39), $P_{GAL1}$*-CDC50 dnf1Δ* (*cdc50Δ dnf1Δ*, YKT1115), $P_{GAL1}$*-CDC50 DNF1-3HA* (*cdc50Δ DNF1-3HA*, YKT1153), and $P_{GAL1}$*-CDC50 dnf1Δ(1465-1571)-3HA* (*cdc50Δ dnf1Δ(1465-1571)-3HA*, YKT1152) strains were streaked onto YPDA plates, incubated for 12 h, and re-streaked onto additional YPDA plates, followed by incubation at 30°C for 2 days. (C) The *dnf1Δ(1465-1571) dnf2Δ* mutant was insensitive to duramycin. Wild-type (YKT39), *dnf1Δ dnf2Δ* (YKT919), *DNF1-3HA dnf2Δ* (YKT1129), and *dnf1Δ(1465-1571)-3HA dnf2Δ* (YKT1130) strains were streaked onto YPDA plates containing 5 μM duramycin, followed by incubation at 30°C for 2 days. (D) The COOH-terminal deletion does not

impair the putative APLT activity of Dnf1p. Strains were grown to the early-mid log phase in YPDA medium at 30°C, followed by labeling with NBD-PE or -PC for 30 min at 30°C. The percentage of average accumulation (±SD, three independent experiments) of NBD-labeled phospholipids for the deletion mutants relative to the wild-type strain is presented. Strains examined are as follows: wild-type (YKT39), *dnf1Δ* (YKT748), *DNF1-3HA* (YKT758), *dnf1Δ(1465-1571)-3HA* (YKT1124), *dnf2Δ* (YKT750), *dnf1Δ dnf2Δ* (YKT919*), DNF1-3HA dnf2Δ* (YKT1129), and *dnf1Δ(1465-1571)-3HA dnf2Δ* (YKT1131).

**Table 1.** *S. cerevisiae* strains used in this study

| Strain[a] | Genotype | Reference or source |
|---|---|---|
| YEF473 | *MAT***a**/α *lys2-801/lys2-801 ura3-52/ura3-52 his3Δ-200/his3Δ-200 trp1Δ-63/trp1Δ-63 leu2Δ-1/leu2Δ-1* | [21] |
| YKT38 | *MAT***a** *lys2-801 ura3-52 his3Δ-200 trp1Δ-63 leu2Δ-1* | [12] |
| YKT39 | *MAT*α *lys2-801 ura3-52 his3Δ-200 trp1Δ-63 leu2Δ-1* | [13] |
| YKT715 | *MAT***a** *lem3Δ::TRP1* | [13] |
| YKT748 | *MAT***a** *dnf1Δ::KanMX6* | [13] |
| YKT750 | *MAT***a** *dnf2Δ::KanMX6* | This study |
| YKT758 | *MAT*α *DNF1-3HA::HIS3MX6* | This study |
| YKT771 | *MAT*α *DNF1-EGFP::KanMX6* | [13] |
| YKT772 | *MAT***a** *cdc50Δ::HIS3MX6 DNF1-EGFP::KanMX6* | [13] |
| YKT773 | *MAT*α *lem3Δ::TRP1 DNF1-EGFP::KanMX6* | [13] |
| YKT787 | *MAT*α *cdc50Δ::HIS3MX6 DNF1-3HA::KanMX6* | This study |
| YKT919 | *MAT*α *dnf1Δ::HphMX4 dnf2Δ::KanMX6* | This study |
| YKT923 | *MAT*α *lem3Δ::TRP1 DNF2-EGFP::KanMX6* | This study |
| YKT935 | *MAT***a** *HIS3MX6::*$P_{GAL1}$*-3HA-CDC50* | This study |
| YKT1056 | *MAT***a** *DNF2-EGFP::KanMX6* | This study |
| YKT1104 | *MAT*α *KanMX6::*$P_{GAL1}$*-3HA-CDC50 lem3Δ::TRP1 crf1Δ::HphMX4* | This study |
| YKT1111 | *MAT*α *lem3Δ::TRP1 dnf2Δ::KanMX6* | This study |
| YKT1112 | *MAT*α *lem3Δ::HphMX4 DNF1-13MYC::KanMX6* | This study |

| | | |
|---|---|---|
| YKT1113 | *MATα lem3Δ::HphMX4 DNF2-13MYC::KanMX6* | This study |
| YKT1115 | *MATα HIS3MX6::$P_{GAL1}$-3HA-CDC50 dnf1Δ::HphMX4* | This study |
| YKT1121 | *MATα cdc50Δ::HIS3MX6 lem3Δ::TRP1 crf1Δ::HphMX4 DNF1-EGFP::KanMX6* pRS316-LEM3 | This study |
| YKT1123 | *MATα dnf1Δ(1465–1572)-EGFP::KanMX6* | This study |
| YKT1124 | *MATα dnf1Δ(1465–1572)-3HA::KanMX6* | This study |
| YKT1129 | *MAT***a** *DNF1-3HA::KanMX6 dnf2Δ::HIS3MX6* | This study |
| YKT1130 | *MATα dnf1Δ(1465-1571)-3HA::KanMX6 dnf2Δ::HIS3MX6* | This study |
| YKT1152 | *MAT***a** *HphMX4::$P_{GAL1}$-3HA-CDC50 dnf1Δ(1465-1571)-3HA::KanMX6* | This study |
| YKT1153 | *MAT***a** *HphMX4::$P_{GAL1}$-3HA-CDC50 DNF1-3HA::KanMX6* | This study |
| YKT1154 | *MAT***a** *HIS3MX6::$P_{GAL1}$-3HA-CDC50 dnf1Δ(1465-1571)-EGFP::KanMX6* | This study |
| YKT1155 | *MAT***a** *HIS3MX6::$P_{GAL1}$-3HA-CDC50 dnf1Δ(1523-1571)-EGFP::KanMX6* | This study |
| YKT1156 | *MAT***a** *HIS3MX6::$P_{GAL1}$-3HA-CDC50 dnf1Δ(1465-1571)-3HA::KanMX6* | This study |
| YKT1157 | *MATα dnf1Δ(1403-1572)-EGFP::KanMX6* | This study |
| YKT1158 | *MATα dnf1Δ(1523-1572)-EGFP::KanMX6* | This study |

[a]YKT strains are isogenic derivatives of YEF473. For YKT strains, only relevant genotypes are described.

**Table 2.** Plasmids used in this study

| Plasmid | Characteristics | Reference or source |
|---|---|---|
| pRS315 | *LEU2 CEN6* | [29] |
| pRS316 | *URA3 CEN6* | [29] |
| YCplac111 | *LEU2 CEN4* | [30] |
| YEplac181 | *LEU2 2μm* | [30] |
| YEplac195 | *URA3 2μm* | [30] |
| pKT1252 [pRS316-LEM3] | *LEM3 URA3 CEN6* | This study |
| pKT1587 [YCplac111-lem3-50] | *lem3-50 LEU2 CEN4* | This study |
| pKT1585 [YCplac111-lem3-112] | *lem3-112 LEU2 CEN4* | This study |
| pKT1586 [YCplac111-lem3-116] | *lem3-116 LEU2 CEN4* | This study |
| pKT1449 [YCplac111-lem3(R316W)] | *lem3(R316W) LEU2 CEN4* | This study |
| pKT1483 [YCplac111-LEM3 ] | *LEM3 LEU2 CEN4* | This study |
| pKT1602 [YEplac195-DNF1] | *DNF1 URA3 2μm* | This study |
| pKT1340 [YEplac181-LEM3] | *LEM3 LEU2 2μm* | This study |

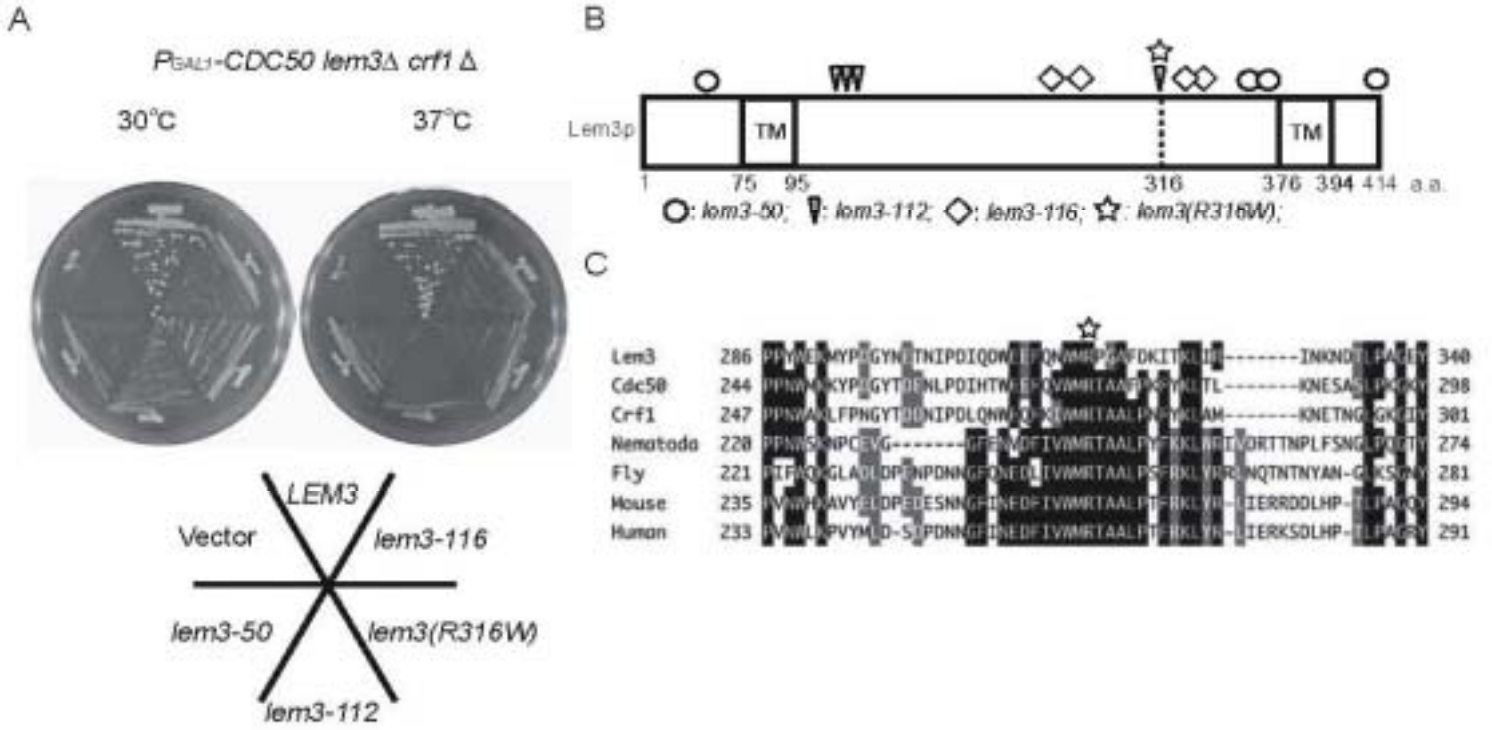
A
PGAL1-CDC50 lem3Δ crf1 Δ
30°C
37°C
LEM3
Vector
lem3-116
lem3-50
lem3(R316W)
lem3-112
B
Lem3p
TM
TM
1
75
95
316
376
394
414
a.a.
○: lem3-50; : lem3-112; ◇: lem3-116; ☆: lem3(R316W);
C
Lem3
Cdc50
Crf1
Nematoda
Fly
Mouse
Human

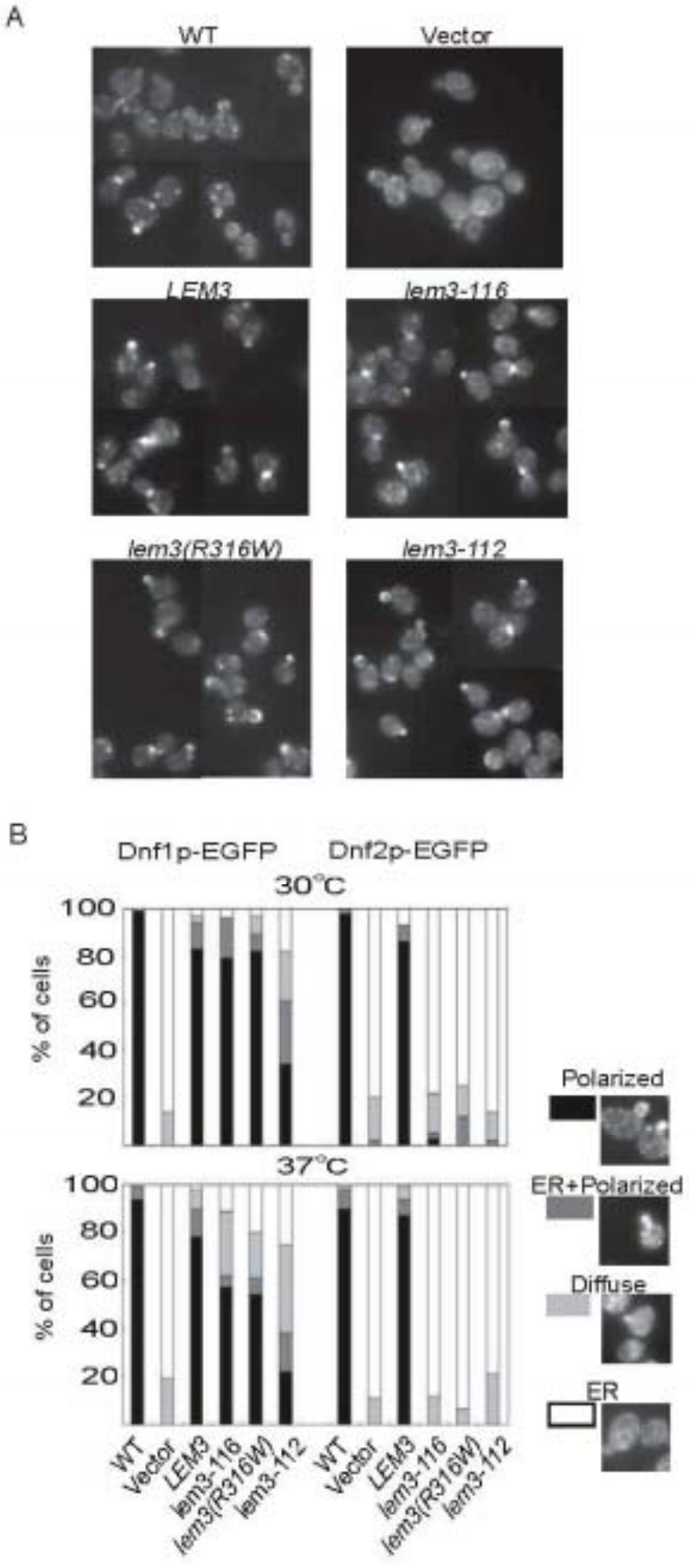
A
WT
Vector
LEM3
lem3-116
lem3(R316W)
lem3-112
B
Dnf1p-EGFP
Dnf2p-EGFP
30°C
37°C
% of cells
100
80
60
40
20
Polarized
ER+Polarized
Diffuse
ER
WT
Vector
LEM3
lem3-116
lem3(R316W)
lem3-112

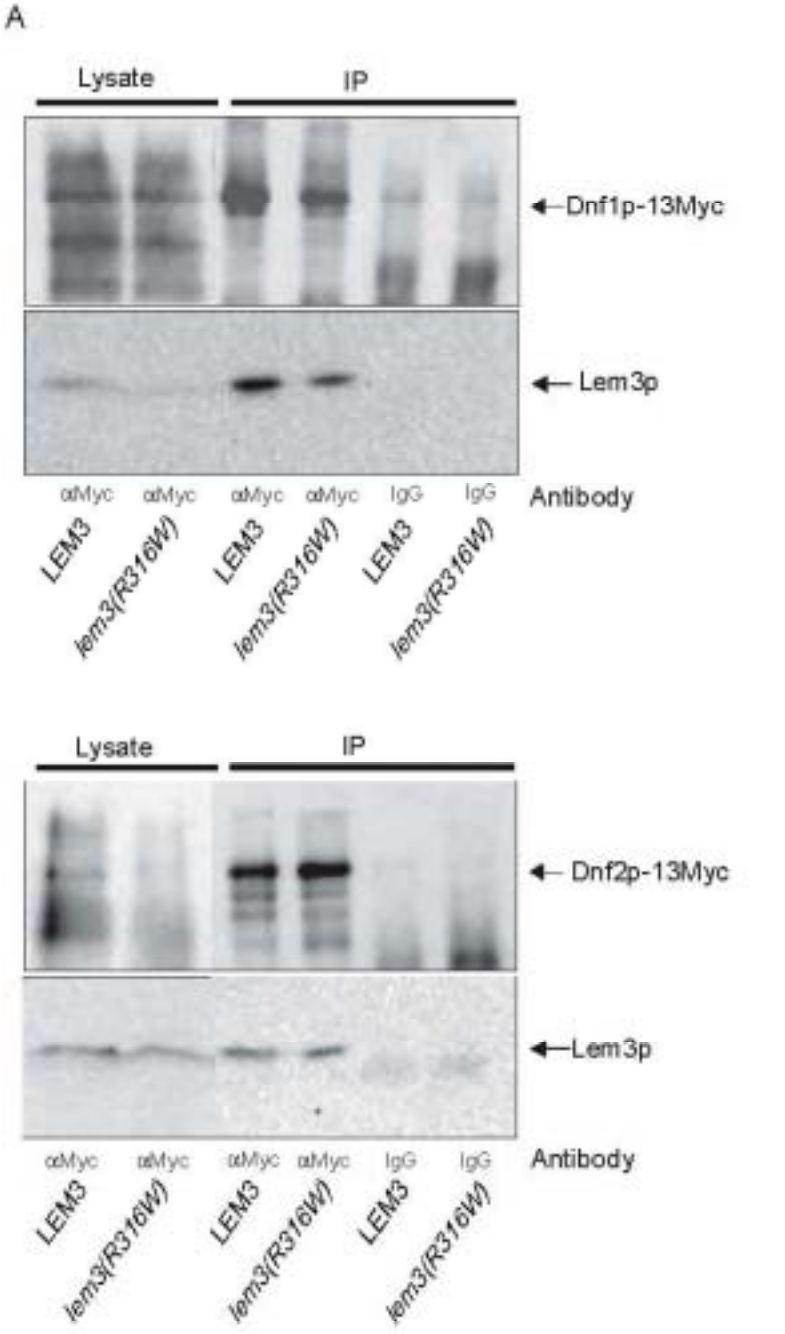
A
Lysate
IP
Dnf1p-13Myc
Lem3p
αMyc αMyc αMyc αMyc IgG IgG
Antibody
LEM3
lem3(R316W)
LEM3
lem3(R316W)
LEM3
lem3(R316W)
Lysate
IP
Dnf2p-13Myc
Lem3p
αMyc αMyc αMyc αMyc IgG IgG
Antibody
LEM3
lem3(R316W)
LEM3
lem3(R316W)
LEM3
lem3(R316W)

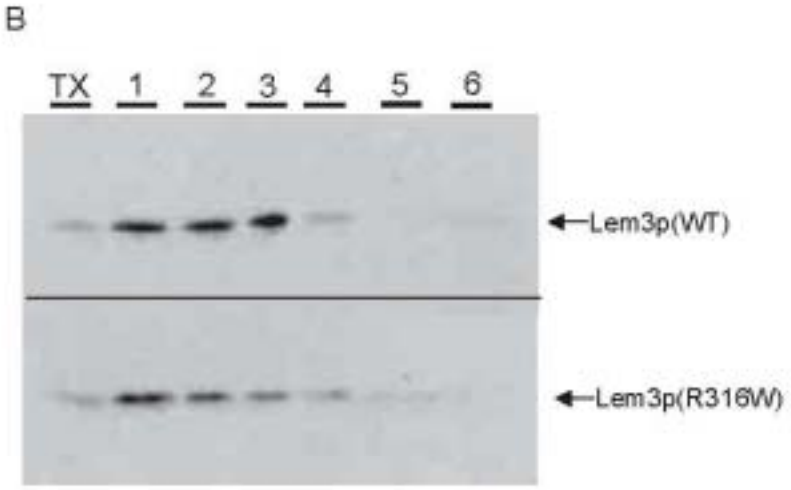
B
TX 1 2 3 4 5 6
Lem3p(WT)
Lem3p(R316W)

A

30°C

| Strains | | Fluorescence (% of wild type) | |
|---|---|---|---|
| | | NBD-PC | NBD-PE |
| *lem3Δ* | + *LEM3* | 100 | 100 |
| *lem3Δ* | + Vector | 13.1 ± 1.9 | 36.6 ± 3.8 |
| *lem3Δ dnf2Δ* | + Vector | 15.0 ± 2.6 | 40.7 ±12.4 |
| *lem3Δ dnf2Δ* | + *LEM3* | 66.8 ± 7.3 | 71.6 ± 7.3 |
| *lem3Δ dnf2Δ* | + *lem3 (R316W)* | 61.4 ± 4.6 | 74.1 ± 3.1 |
| *lem3Δ dnf2Δ* | + *lem3-112* | 48.5 ± 6.2 | 52.5 ± 7.5 |

37°C

| Strains | | Fluorescence (% of wild type) | |
|---|---|---|---|
| | | NBD-PC | NBD-PE |
| *lem3Δ* | + *LEM3* | 100 | 100 |
| *lem3Δ* | + Vector | 18.3 ± 3.5 | 29.3 ± 2.8 |
| *lem3Δ dnf2Δ* | + Vector | 20.5 ± 2.0 | 34.5 ± 5.5 |
| *lem3Δ dnf2Δ* | + *LEM3* | 63.9 ±14.4 | 68.2 ±10.9 |
| *lem3Δ dnf2Δ* | + *lem3 (R316W)* | 67.8 ±10.6 | 65.9 ±17.8 |
| *lem3Δ dnf2Δ* | + *lem3-112* | 46.1 ± 9.5 | 28.3 ± 3.9 |

B

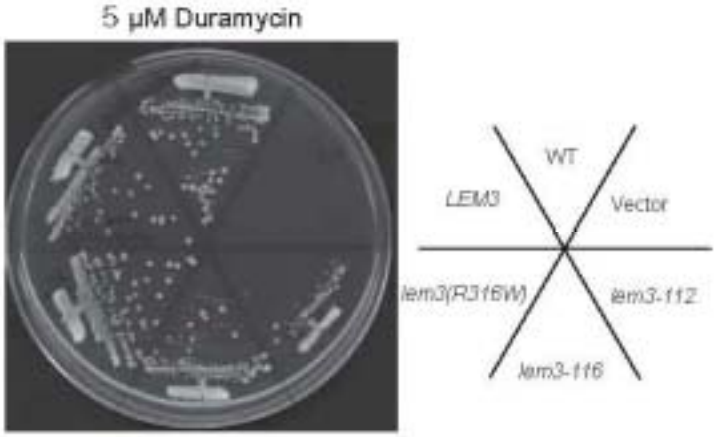

A

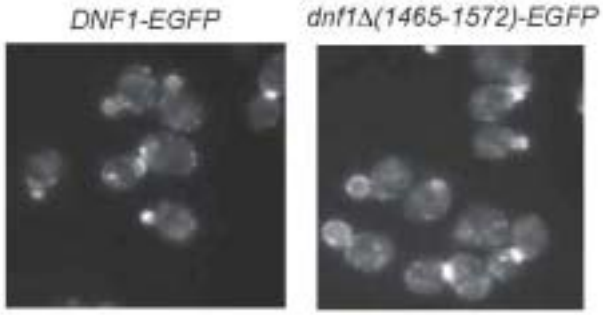


B

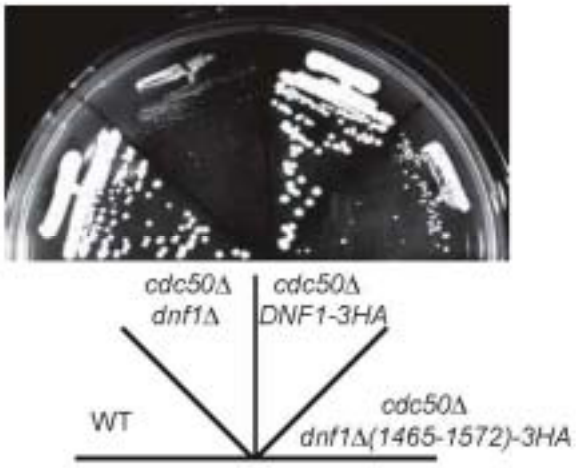


C


D

| Strains | Fluorescence (% of wild type) | |
|---|---|---|
| | NBD-PC | NBD-PE |
| WT | 100 | 100 |
| *dnf1Δ* | 90.8 ± 4.8 | 85.8 ± 4.8 |
| *DNF1-3HA* | 97.6 ± 1.2 | 99.8 ± 7.3 |
| *dnf1Δ (1465-1572)-3HA* | 99.8 ± 2.7 | 97.8 ± 6.2 |
| *dnf2Δ* | 43.2 ± 0.8 | 49.4 ± 3.5 |
| *dnf1Δ dnf2Δ* | 14.4 ± 2.0 | 22.7 ± 2.8 |
| *DNF1-3HA dnf2Δ* | 37.8 ± 1.5 | 47.3 ± 2.3 |
| *dnf1Δ (1465-1572)-3HA dnf2Δ* | 59.3 ± 2.0 | 65.5 ± 5.9 |

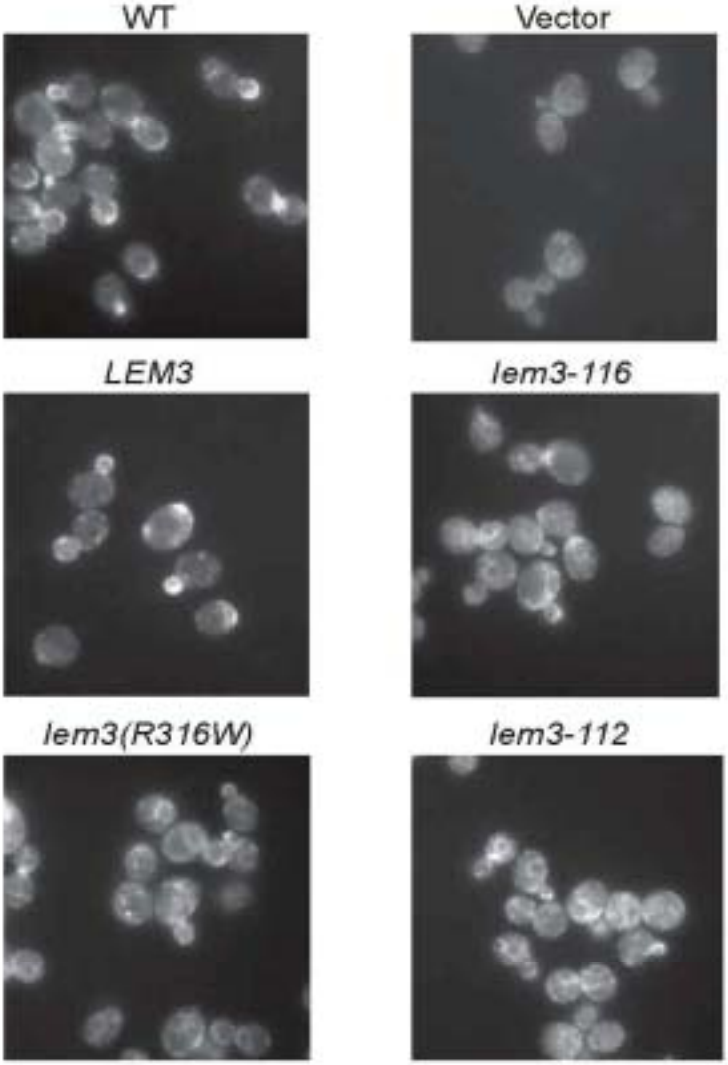
WT
Vector
LEM3
lem3-116
lem3(R316W)
lem3-112

A


B

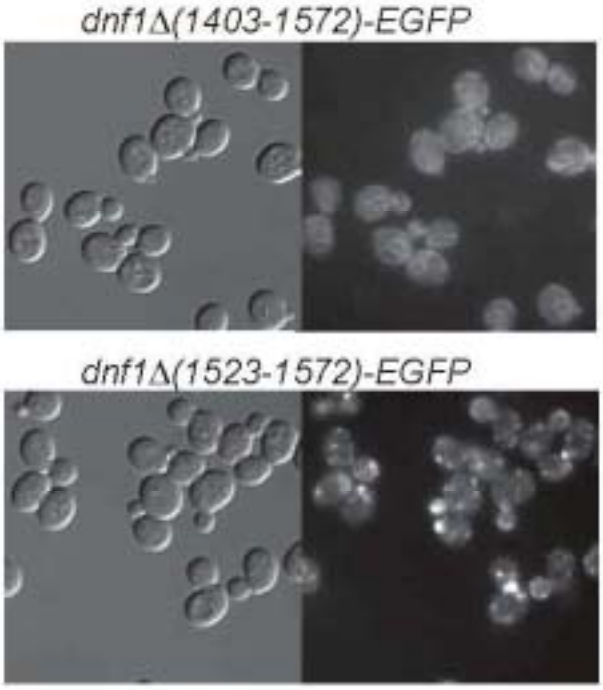


C

| Strains | Tag | |
|---|---|---|
| | *-3HA* | *-EGFP* |
| *cdc50Δ DNF1* | +++ | +++ |
| *cdc50Δ dnf1Δ(1465-1572)* | + | + |
| *cdc50Δ dnf1Δ(1523-1572)* | +++ | + |

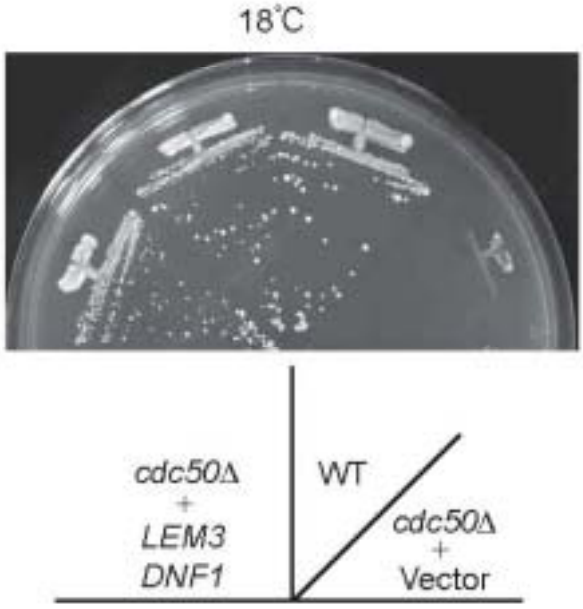
18°C
cdc50Δ
+
LEM3
DNF1
WT
cdc50Δ
+
Vector